Received: 16 August 2022 | Revised: 7 November 2022 | Accepted: 22 December 2022

DOI: 10.1111/ijag.16622

INTERNATIONAL JOURNAL OF Applied Glass SCIENCE

RESEARCH ARTICLE

Case II diffusion of water in Na_2O–$3SiO_2$ glass: Constant tensile stress gradient at the diffusion interface

Bronson D. Hausmann | **Minoru Tomozawa**

Department of Materials Science and Engineering, Rensselaer Polytechnic Institute, Troy, New York, USA

Correspondence
Minoru Tomozawa, Department of Materials Science and Engineering, Rensselaer Polytechnic Institute, Troy, NY 12180, USA.
Email: tomozm@rpi.edu

Funding information
NSF, Grant/Award Number: DMR-1713670; Corning Inc.

Abstract

Some polymers and oxide glasses exhibit unusual diffusion of liquid or gas, with the depth of diffusion exhibiting a linear increase with time, instead of normal square root of time dependence. There have been many models, but very few experimental data that can help clarify the cause of the phenomenon's existence in glass. Residual stress in sodium trisilicate glass (Na_2O–$3SiO_2$) samples was characterized following Case II water diffusion at 80°C in a saturated water vapor environment. The surface-swelled layer of the glass was removed by dissolving it in water, and birefringence of the newly revealed surface layer was measured. The presence of a constant negative tensile stress gradient was revealed by indicating that Case II diffusion in sodium trisilicate glass originates from this stress gradient, which overwhelms the more typical Fick's law concentration-dependent flux.

KEYWORDS
birefringence, characterization, diffusion, optical properties, silicate, theory

1 | INTRODUCTION

Water diffusion in sodium trisilicate glasses with various quantities of water contents has been previously investigated, with particular interest in the effects of water in glass on diffusivity and conductivity of sodium ions in the material.[1–5] Tomozawa and Molinelli have previously concluded that below a certain temperature and depending on water content of the original glass, water transport does not follow the expected Fick's law behavior.[4] Instead water diffusion was described by what Alfrey et al.[6] originally referred to as Case II diffusion (Figure 1A,B). Case II diffusion occurs when there exists a step-like concentration profile that progresses through the material at a constant rate, with the concentration front linearly progressing with time.[7] This is in contrast to Fick's law, which predicts a complementary error function profile that progresses linearly with the square root of time (Figure 1B).[7]

Crank[7] paraphrased Alfrey et al.'s[6] statement of Case I (Fickian) diffusion and Case II diffusion (no-Fickian) diffusion as follows:

(i) Case I or Fickian diffusion in which the rate of diffusion is much less than that of relaxation.
(ii) Case II diffusion the other extreme in which diffusion is very rapid compared with the relaxation processes.

Several theories have been developed to model possible mechanisms of Case II diffusion, with particular focus on the phenomenon that happens during solvent diffusion into glassy polymers. Crank proposed that Case II behavior can be modeled as a concentration-dependent

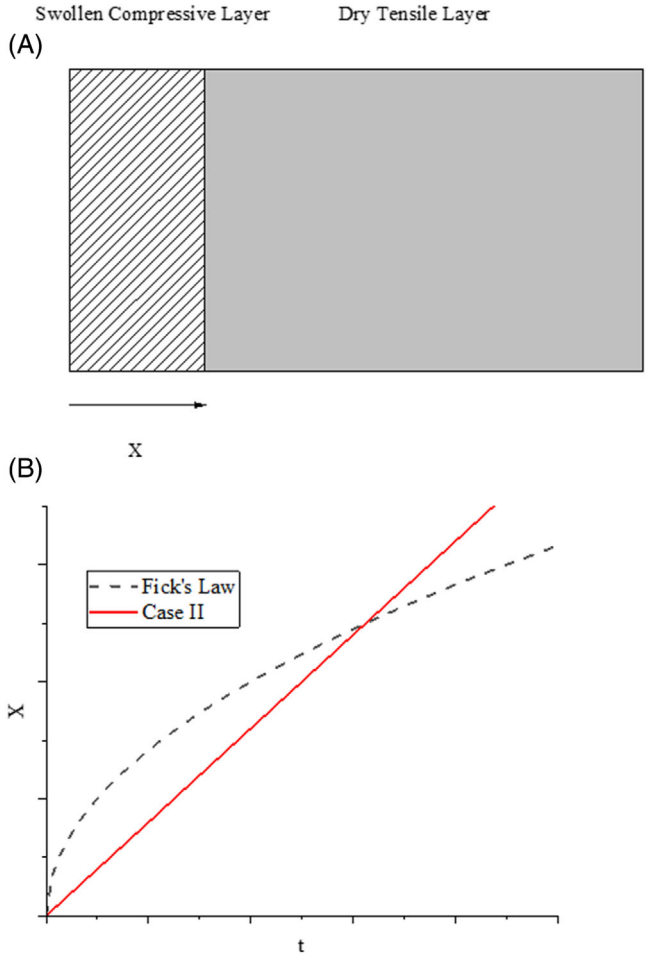

FIGURE 1 (A) Schematic of typical diffusion front progression of Case II diffusion, showing the interface progression at point, X. A constant diffusion velocity is maintained by the presence of compressive stress in the hydrated layer and tensile stress in the unreacted "dry" interior. (B) Schematic curves describing Case II and Fick's law diffusion front progression, X, as a function of time. Case II diffusion is observed to progress linearly with time, whereas Fick's law predicts square root time dependence.

diffusivity, with a diffusion interface that can be predicted by an additional linear constant upon the boundary progression expected of Fick's law[8,9]:

$$X = k \cdot \sqrt{Dt} \tag{1}$$

where k is a constant determined for the material and experimental conditions, D is the diffusivity of the solvent, and t is time.

It was later suggested by Wang et al.[10] that a rule of mixing be applied to determine the Case II and Fickian contribution to diffusion:

$$X = 2k \cdot \sqrt{Dt} + vt \tag{2}$$

where v is a term relating to the stress gradient within the polymer as well as the general mobility of the penetrating species, both of which were thought to be relevant to the dominance of Case II behavior in polymer–solvent systems.

A similar theory was developed by Cox and Cohen[11] which proposed that the modification of the flux within the material included a linear dependency upon the stress gradient at the interface:

$$J = -\frac{\partial \mu}{\partial C} \cdot \nabla C - \frac{\partial \mu}{\partial \sigma} \cdot \nabla \sigma \tag{3}$$

where J is the flux in the material, μ is the chemical potential, C is the concentration, and σ is the stress within the plane where the flux is being measured, most notably near the diffusion interface. A similar, more general consideration has been suggested for diffusion in the presence of any external potential by Shewmon, with similar applicability[12]:

$$J = -D \cdot \left(\nabla C + \frac{C \nabla V}{kT} \right) \tag{4}$$

where V is a general applied potential, including stress, and k is the Boltzmann constant. Inspection of Equations (3) and (4) allows a comparison between Cox and Cohen's stress gradient prediction and Shewmon's potential, leading to

$$\nabla \sigma \propto \frac{\nabla V}{kT} \tag{5}$$

It is thus expected that the effect of the stress gradient is likewise thermally activated, similar to any other potential gradient effect upon the flux. Although previous studies of sodium trisilicate glass have proposed that such an effect on water transport may be occurring, these observations relied solely on diffusion depth measurements with no available stress data. Instead, the authors had proposed an empirical model very similar to Equation (2).[5]

The conception of the stress dependence of flux at the interface is of interest as the stress in a material, such as sodium trisilicate glass, is measurable using photoelastic techniques, allowing for experimental confirmation in a manner that is difficult to obtain for a polymer/solvent system. This work therefore investigates the water diffusion behavior of sodium trisilicate glass while concurrently measuring the residual stress profiles at the diffusion interface in order to determine if the origin of Case II diffusion behavior in the material can be described by the model developed via Equations (3) and (4).

Furthermore, oxide glasses exhibit large stress relaxation (delayed elasticity) due to impurity water in glass,[13]

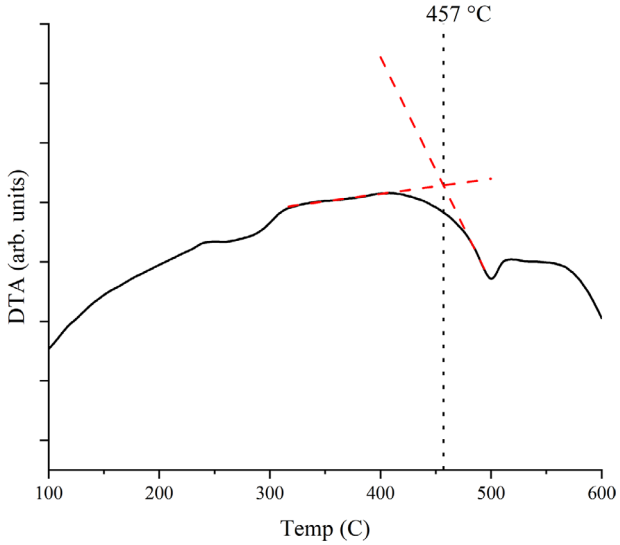

FIGURE 2 Differential therman analysis (DTA) curve depicting the glass transition temperature estimate from the change in heat of the glass sample. T_g value agrees with a sodium trisilicate glass containing approximately .1 wt.% water.[3]

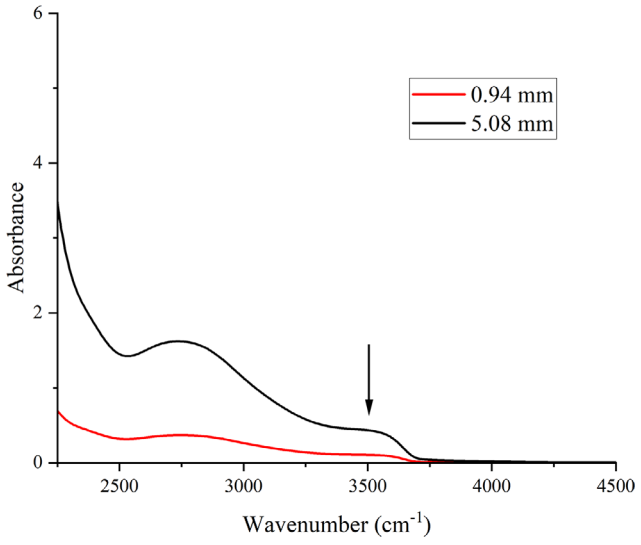

FIGURE 3 Fourier transform infrared (FTIR) spectrum of two samples of sodium trisilicate glass polished to the indicated thickness. Water content was estimated to be 800 ± 50 wt. ppm using a practical extinction coefficient of 24 ± 3 L mol^{-1} cm^{-1} for the 3500 cm^{-1} band as previously determined by Acocella.[15] The relevant band is indicated by the arrow for both spectra.

and this would enable one to measure stress near the diffusion front, even after eliminating a swollen layer.

2 | EXPERIMENTAL PROCEDURES

Sodium trisilicate glass, received as a large crucible pour (Corning Inc.), was cut into cubic pieces with roughly 1 cm in edge length before surface preparation. These were then annealed at 500°C for 1 h before furnace cooling. The annealing temperature was measured with differential thermal analysis (DTA) using a powdered sample (Figure 2) as has been measured for the same material previously.[14] A T_g of 457°C was found, indicating that 500°C was sufficient for the removal of residual stress. This T_g value was likewise found to be in good agreement with the estimated as-received water content of 800 ± 50 wt. ppm, as determined by absorption measurements made using Fourier transform infrared (FTIR) spectroscopy (Figure 3).[15] This method uses the IR absorption at a specific wavelength associated with water in the glass via the Beer–Lambert law to determine the water content,

$$C_{H_2O} = A/\left(\varepsilon_{pract} \cdot y\right) \quad (6)$$

where C_{H_2O} is the water concentration in (mol L^{-1}), A is absorbance, ε_{pract} is the practical extinction coefficient in (L mol^{-1} cm^{-1}), and y is the material thickness. The value of the practical extinction coefficient of water in sodium trisilicate glass has been obtained previously as 24 ± 3 L mol^{-1} cm^{-1}.[15]

Surfaces of the annealed samples were polished using finer silicon carbide paper in steps of 240, 400, 600, and 1200 grit before a final polish of cerium oxide in distilled water. After polishing, samples were etched in a solution of 5% HF and 10% H_2SO_4 for 30 s. At this stage, the dimensions of the samples were measured using an optical microscope, Nikon Eclipse LV100N POL, to find cubes with edge length 4.9 ± .1 and 6.7 ± .2 mm. The larger edge length cubes were used for longer time heat treatments, so that the opposite face's diffusion front remained sufficiently distant.

Samples were heat-treated at 80°C in a 355 torr (47.3 kPa) saturated water vapor environment. In order to maintain this vapor pressure, samples were placed within a sealed PTFE container and suspended over a reservoir of deionized water (Figure 4). Following successively increasing heat-treatment times, 4, 6, 12, 24, 48, and 96 h, samples were removed from the reservoir, and the hydrated surfaces were readily dissolved by room temperature water. The new dimensions of the sample, indicated by arrows in Figure 4, were then measured and compared to the pretreated sample to find the depth of the diffusion interface.

In addition to the depth of hydration, the residual stress in the remaining sample was characterized via birefringence measurement, using previously developed photoelastic techniques employed by the same microscope used for dimensioning of the sample.[16–19] The Sènarmont method[20] was used to measure relative retardation, the phase shift in polarized light passing through the sample in

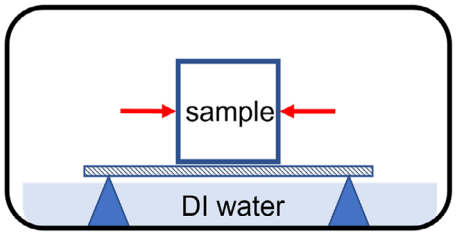

FIGURE 4 Schematic of sample configuration during heat treatment. Interface depth and stress were measured along the dimension indicated by arrows. Although water diffusion/reaction proceeds in all surfaces, significantly large sample assures that edge effects are minimized. Samples are suspended above deionized water, upon a silica glass plate, within a sealed polytetrafluoroethylene (PTFE) vessel to ensure saturated vapor pressure during the treatment.

degrees, as a function of distance from the diffusion front into the unreacted glass (Figure 5):

$$\delta(x) = 360° \cdot \frac{\Delta(x)}{\lambda} \tag{7}$$

where δ is relative retardation in degrees, Δ is retardance in nm, the phase shift of the propagating polarized light, and λ is the wavelength of the light used during measurement (546 nm). The optical configuration used in the Sènarmont method is such that rotation of the microscope analyzer that results in a minimal intensity is related to the relative retardation:

$$\delta(x) = 2 \cdot \theta_{\min}(x) \tag{8}$$

where $\theta_{\min}(x)$ is the analyzer angle that produces minimal intensity as a function of position within the sample. The measured intensities captured by a CMOS camera attached to the microscope were used to obtain intensity values. Such intensity values were used to calculate $\theta_{\min}$ for use in Equations (7) and (8), in order to calculate the stress profile. The precision of this method is limited by the wavelength of the quarter wave plate and the precision of the rotation of the analyzer. For this work, spatial precision was limited to $\pm.48\ \mu$m, whereas retardance was limited to $\pm.3$ nm.

2.1 | Retardance is related to stress in the glass by the stress optic law[21,22]

$$\sigma = \frac{\Delta}{C \cdot y} \tag{9}$$

where σ is stress in MPa, Δ is retardance in nm, C is the stress optical coefficient in Brewster (10^{-12} Pa^{-1}), and y is the thickness of the measured material in mm. Results are reported as birefringence (Δ/y) alongside approximate equivalent stress. The stress optic coefficient variation with water content ahead the hydrated interface is expected to be small.[23] It is also likely that the effect upon stress optic coefficient is consistent across all heat-treated samples.

To avoid the interference of thermal expansion differences due to the change in temperature, a heated microscope stage (Bioscience Tools) was employed to perform the stress measurement at 80°C in lab air (Figure 6). The relatively low partial pressure of water assured the negligible hydration of the newly exposed unreacted surface during the measurement. Likewise, stress measurement at the chosen furnace temperature would assure that all residual stress was a result of the heat treatment and hydration itself as opposed to the subsequent cooling of the sample. The collected residual stress profiles were then compared to existing models for Case II diffusion in order to discern if evidence for a clear mechanism existed in the measured stress and theorized water concentration profiles.

3 | RESULTS

From 4 to 48 h, the diffusion distance of the hydrated layer of the glass was found to progress linearly with time at a rate of $4.67 \pm .23\ \mu$m h^{-1} (Figure 7). As this interface moved deeper, a residual tensile stress was found consistently within a short distance from the newly created surface of the glass with the stress sharply increasing. Tensile stress initially increased with the depth near the surface and then decreased gradually for each sample (Figure 8).

4 | DISCUSSION

The observed tensile residual stress is consistent with what is expected for a stress relaxation of the glass subjected to a tensile stress by the swollen surface layer, after the removal of surface layer. There are other parallels that can be drawn to Thomas and Windle; namely, the conception of the stress component of diffusion being directly correlated to the creep behavior of the material.[24] The magnitude of tensile stress decreases with time, similar to assumptions within Cox and Cohen's original derivation in which a standard linear model is assumed for viscoelastic stress relaxation.[11] Slightly lower value of the tensile stress with increasing heat-treatment time (or diffusion distance) shown in Figure 8 may also be caused by the longer time required for removal of the thicker swollen layer before birefringence measurement. This can cause a slight reduction of the residual stress by relaxation in reality.

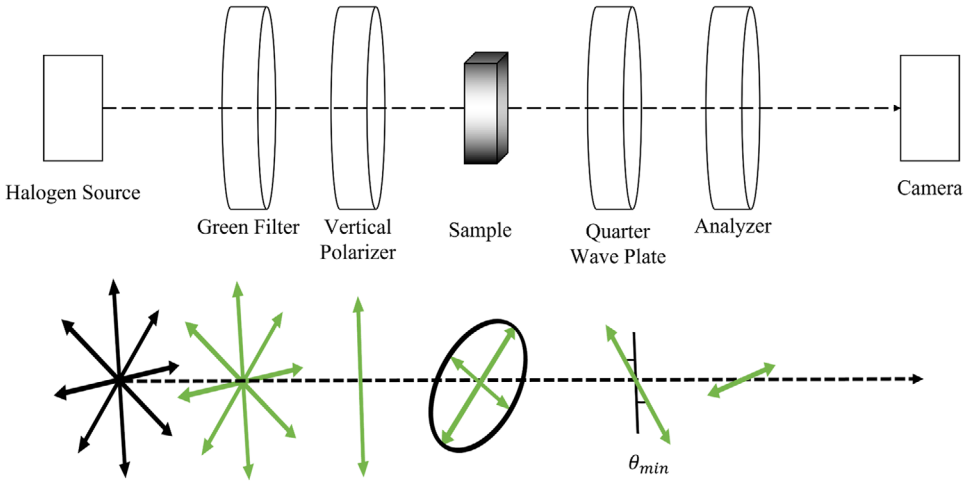

FIGURE 5 Schematic of the optical configuration used for retardance measurement of the sample, alongside the light polarization as it passes through each element. Light intensity is measured as a function of microscope analyzer angle to determine the angle of minimum intensity θ_{min}. At this angle, the retardation δ is proportional to θ_{min} via Equation (8) and is used with Equation (7) to find the retardance, Δ.

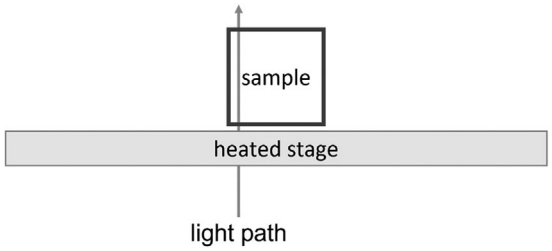

FIGURE 6 Schematic of the heated stage in relation to the incident light of the microscope and the sample, used for birefringence measurement

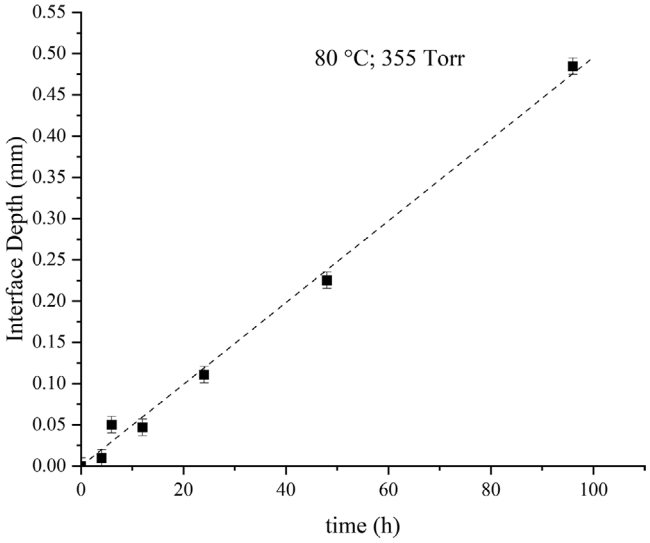

FIGURE 7 Diffusion interface depth versus time for water in sodium trisilicate at 80°C saturated water vapor. Fit is linear with an intercept of zero and rate of $4.67 \pm .23\ \mu m\ h^{-1}$.

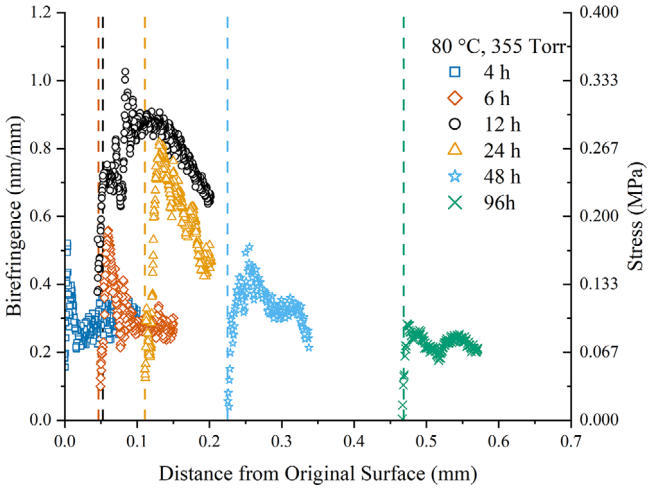

FIGURE 8 Residual stress profiles on the unreacted side of the diffusion interface in $Na_2O{\cdot}3SiO_2$ glass samples after for 4–96 h at 80°C treatment in water vapor. Maximum stress magnitude occurs following the 12 h heat treatment. The vertical dashed lines represent the surfaces of the glass sample after the swollen layer was washed away.

It has previously been found that Case II diffusion behavior was observed in sodium trisilicate glass as a function of temperature and water content well below the glass transition temperature (Figure 9).[4,5] The demarcation between Case II and Fick's law behavior thus likely corresponds to the point at which the effective stress relaxation time becomes longer than the transport, and reaction of water in the glass and residual stress starts to become important. Previously, this was assembled via data obtained in a manner identical to that seen in Figure 7, but the cause of this demarcation in diffusion mechanism was at the time unexplained.

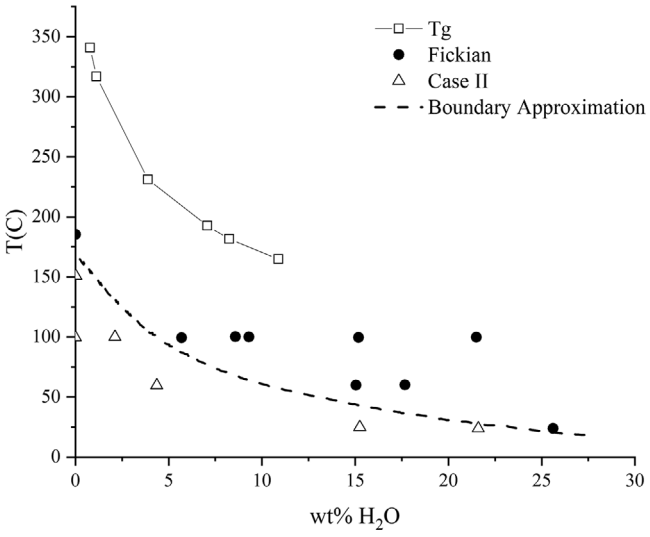

FIGURE 9 Comparison of dominant diffusion behavior in sodium trisilicate glass as a function of temperature and water content of the unreacted glass. The dependence of T_g with water content is also included. *Source*: Data collected by Tomozawa and Molinelli[4]

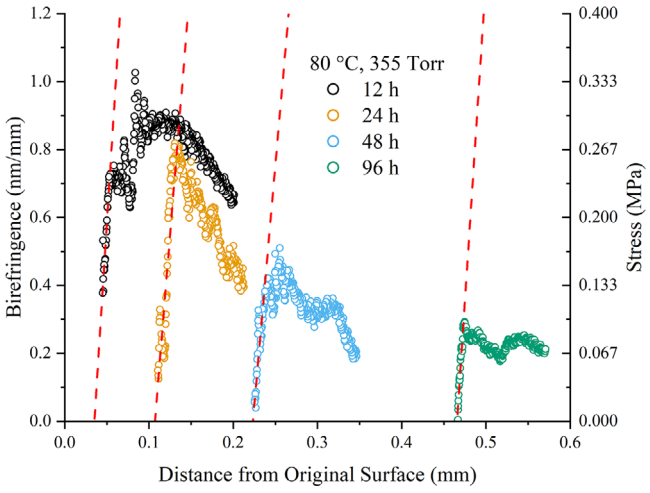

FIGURE 10 Retardance profiles from 12 to 96 h displaying nearly identical initial slopes (dashed line) from the surface inward. The data was fit to an average slope of .014 ± .009 MPa mm^{-1}, or .0341 nm mm^{-2}.

In addition, noteworthy is the slope of the residual stress profile at the surface of each sample is very consistent for different heat-treatment times (.037 ± .006 MPa mm^{-1}) (Figures 10 and 11, and Table 1 second column). This opposite slope of the surface layer to the deeper part of the residual stress is due to fast surface stress relaxation in the presence of water or water vapor, similar to the fast surface stress relaxation[25] (see Figure A2 of Ref. [25]). This surface relaxation happens only after the surface layer was eliminated. During the Case II diffusion process, the residual stress at the water diffusion front is expected to be given by the solid line in Figure 11, with a sharp negative slope. From the consistent slope of the surface-relaxed residual stress, after the removal of the surface water diffusion front, the same water flux is expected at different depths, the characteristic of Case II diffusion.

TABLE 1 Stress gradient linear fit values before and after interior maximum from 4 to 96 h

Heat-treatment time (h)	Slope before interior max (MPa mm^{-1})	Slope after interior max (MPa mm^{-1})
4	.065 ± .004	−.0076 ± .002
6	.048 ± .003	$-.0053 \pm 6.27 \times 10^{-4}$
12	.039 ± .004	$-.0028 \pm 2.65 \times 10^{-5}$
24	.031 ± .003	$-.0044 \pm 7.4 \times 10^{-5}$
48	.028 ± .002	$-.0021 \pm 6.97 \times 10^{-5}$
96	.038 ± .002	$-.0017 \pm 7.04 \times 10^{-5}$

Because the interface moves at a constant velocity during heat treatment, it is to be expected that each interface experiences the same degree of surface stress relaxation upon the removal of the reacted gel layer, which accounts for the deviation between the observed and predicted stress profiles (Figure 12). The consistency of this surface relaxation also affirms the consistency of the experimental procedure that the removal of the reacted layer removes all residual compressive stress as well as some portion of a presumed equal and opposite elastic tension, leaving only the viscoelastic tension that is measured. The negative stress gradient beyond the relaxation at the surface of the interface (directly following the subsurface stress maximum) is similar to that predicted for a residual stress effect on the flux, as has been theorized in analogous polymer/solvent systems by Cox and Cohen.[11,26] This stress profile would again likely be antisymmetric about the interface with a sharp compressive stress within the reacted layer during the diffusion process and has the observed interior maximum due to the removal of the reacted layer. A work done by Thomas and Windle that performed the complementary experiment to that performed here, namely, measuring the residual stress in the reacted layer of a Case II material (via methanol diffusion in PMMA), found a compressive stress profile near the interface as is predicted for this situation.[27]

A linear fit of the residual stress gradient beyond the interior stress maximum was made and was found to decay relatively quickly first, then significantly more slowly after about 12 h (Table 1). The slow decay of the negative stress gradient indicates that the diffusion is likely approach Fick's law behavior at very long times, as predicted by Cox and Cohen (Table 1). These observations agree with the behavior predicted by Equations (3) and (4) and strongly suggest that for sodium trisilicate glass, Case II diffusion

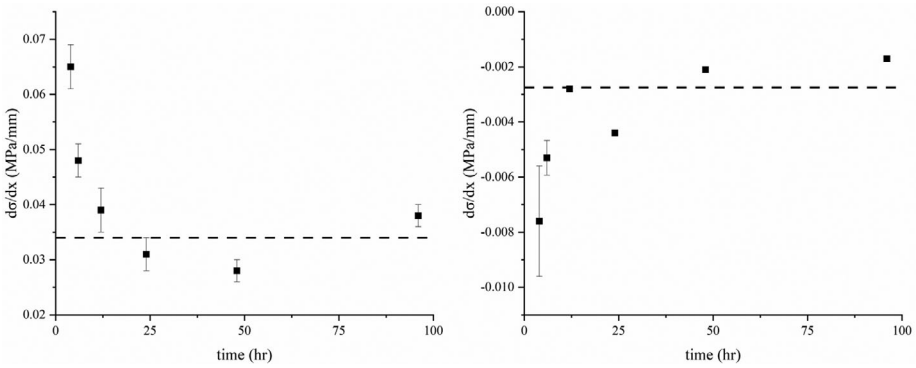

FIGURE 11 Graphical representation of the results presented in Table 1. The stress gradient at the diffusion interface (left) as well as the stress gradient from the interior maximum inward (right) approach a steady state following initial hydration of the glass surface.

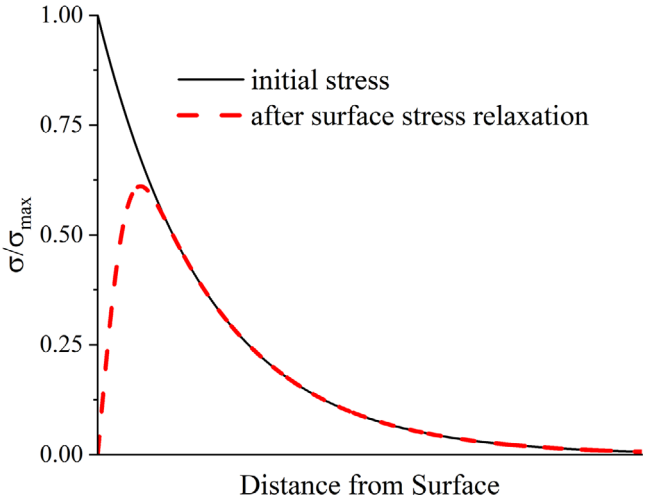

FIGURE 12 Schematic of the stress at the water diffusion front as-expected (solid line) and as-observed (dotted line) with surface stress relaxation. This relaxation accounts for the positive stress gradient that is observed at the unreacted glass surface.[25] A negative gradient is to be expected if there were no relaxation, as indicated by the solid curve.

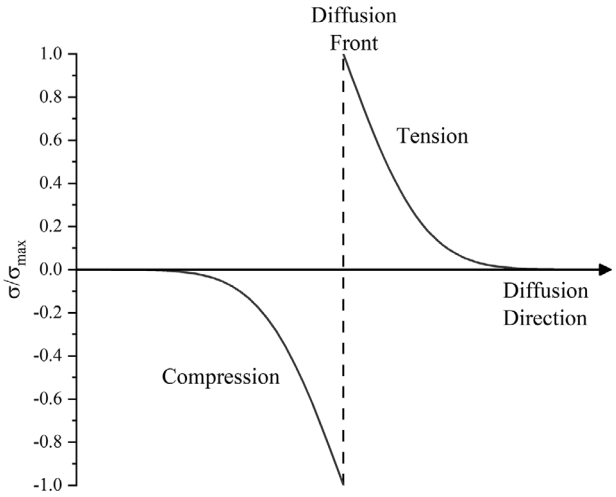

FIGURE 13 Schematic residual stress at the interface of Case II diffusion front. Left-hand side of the interface has compressive stress and right-hand side of the interface has tensile stress.

is originated via the tensile stress gradient at the diffusion front.

Combing the compressive stress layer of the swollen side by Thomas and Windle[27] with the present results on tensile stress of unswollen side, the stress profile during the Case II diffusion front is expected as shown in Figure 13, where the left-hand side represents compressive stress in the swollen surface, and the right-hand side represents tensile stress in front of the diffusion interface. The compressive stress behind the interface is responsible for the diffusion pattern of a step function type, and the tensile stress in front of the interface is responsible for a constant diffusion flux at the interface. To obtain Case II diffusion, with a constant diffusion flux and a step function of diffusion profile, the residual stress profile has to be time independent.

5 | CONCLUSIONS

Residual stress at the water diffusion interface of $Na_2O{\cdot}3SiO_2$ glass has been measured as a function of successive low-temperature heat treatment in a saturated water vapor atmosphere. Case II diffusion was found to occur, with a steady-state tensile stress gradient found at the interface likely resulting from surface stress relaxation. Beyond the surface relaxation, the negative stress gradient is seen to remain nearly constant while slowly decreasing with heat-treatment time. This agrees with the models proposed for Case II diffusion in glassy polymers where structural relaxation is seen to result in Fick's law diffusion at long times. The fact that a residual stress arises within

the unreacted glass network likewise agrees with both the expected pressure profile predicted for solvents in glassy polymers, as well as with the previously observed diffusion/reaction behavior of molecular water within silicate glasses. The tensile stress gradient beyond the diffusion interface agrees with predictions of the stress dependence of flux in the material by Cox and Cohen, indicating that the negative tensile stress gradient is the origin of Case II diffusion in sodium trisilicate glass.

ACKNOWLEDGMENTS

This work was supported by NSF grant DMR-1713670 and by Corning Inc.

ORCID

Bronson D. Hausmann https://orcid.org/0000-0003-1448-3392

REFERENCES

1. Molinelli J, Tomozawa M, Takata M. Sodium transport in the Na_2O–H_2O–SiO_2 glass system. J Am Ceram Soc. 1985;68(3):165–8. https://doi.org/10.1111/j.1151-2916.1985.tb09658.x
2. Takata M, Acocella J, Tomozawa M, Watson EB. Effect of water content on the electrical conductivity of Na_2O–$3SiO_2$ glass. J Am Ceram Soc. 1981;64(12):719–4. https://doi.org/10.1111/j.1151-2916.1981.tb15894.x
3. Tomozawa M, Takata M, Acocella J, Watson EB, Takamori T. Thermal properties of $Na_2O{\cdot}3SiO_2$ glasses with high water content. J Non-Cryst Solids. 1983;56(1):343–8. https://doi.org/10.1016/0022-3093(83)90491-X
4. Tomozawa M, Molinelli J. Non-Fickian diffusion of water in glass. Riv della Staz Sper Vetro. 1984;1(5):33–7.
5. Tomozawa M, Ito S, Molinelli J. Hygroscopicity of glasses with high water content. J Non-Cryst Solids. 1984;64(1–2):269–8. https://doi.org/10.1016/0022-3093(84)90222-9
6. Alfrey T, Gurnee EF, Lloyd WG. Diffusion in glassy polymers. J Polym Sci C: Polym Symp. 1966;12(1):249–1. https://doi.org/10.1002/polc.5070120119
7. Crank J. The mathematics of diffusion. Oxford University Press; 1975.
8. Crank J, Park GS. Diffusion in high polymers: some anomalies and their significance. Trans Faraday Soc. 1951;47:1072–84.
9. Crank J. A theoretical investigation of the influence of molecular relaxation and internal stress on diffusion in polymers. J Polym Sci. 1953;11(2):151–8. https://doi.org/10.1002/pol.1953.120110206
10. Wang TT, Kwei TK, Frisch HL. Diffusion in glassy polymers. III. J Polym Sci A-2: Polym Phys. 1969;7(12):2019–28. https://doi.org/10.1002/pol.1969.160071204
11. Cox RW, Cohen DS. A mathematical model for stress-driven diffusion in polymers. J Polym Sci B: Polym Phys. 1989;27(3):589–2. https://doi.org/10.1002/POLB.1989.090270308
12. Shewmon P. Diffusion in solids. Cham: Springer International Publishing; 2016. https://doi.org/10.1007/978-3-319-48206-4
13. Zdaniewski WA, Rindone GE, Day DE. The internal friction of glasses. J Mater Sci. 1979;14(4):763–5. https://doi.org/10.1007/BF00550707
14. Tomozawa M, Takata M, Acocella J, Watson EB, Takamori T. Glass transition temperature of Na_2O * $3SiO_2$ glasses with high water content. Yogyo KyokaiShi/J Ceram Soc Jpn. 1983;91(8):377–3.
15. Acocella J. The nature of dissolved water in sodium silicate glasses and its effect on various properties. Troy, NY: Rensselaer Polytechnic Institute; 1983.
16. Hausmann BD, Miller PA, Aaldenberg EM, Blanchet TA, Tomozawa M. Modeling birefringence in SiO_2 glass fiber using surface stress relaxation. J Am Ceram Soc. 2020;103(3):1666–76. https://doi.org/10.1111/jace.16900
17. Hausmann BD, Aaldenberg EM, Tomozawa M. Photoelastic confirmation of surface stress relaxation in silica glasses: fiber bending and rod torsion. J Am Ceram Soc. 2021;104(7):3087–96. https://doi.org/10.1111/jace.17690
18. Chu PL, Whitbread T. Measurement of stresses in optical fiber and preform. Appl Opt. 1982;21(23):4241. https://doi.org/10.1364/AO.21.004241
19. Jessop HT. On the Tardy and Sènarmont methods of measuring fractional relative retardations. Br J Appl Phys. 1953;4(5):138–1. https://doi.org/10.1088/0508-3443/4/5/303
20. De Sènarmont H. Sur les modifications que la réflexion spéculaire à la surface des corps métalliques imprime à un rayon de lumière polarisée. Ann Chim Phys. 1840;73:337–2.
21. Lagakos N, Mohr R, El-Bayoumi OH. Stress optic coefficient and stress profile in optical fibers. Appl Opt. 1981;20(13):2309. https://doi.org/10.1364/AO.20.002309
22. Brewster D. On the laws which regulate the polarisation of light by reflexion from transparent bodies. Philos Trans R Soc London. 1815;105:125–9.
23. Acheroy S, Merken P, Geernaert T, Ottevaere H, Thienpont H, Berghmans F. Algorithms for determining the radial profile of the photoelastic coefficient in glass and polymer optical fibers. Opt Exp. 2015;23(15):18943–54. https://doi.org/10.1364/OE.23.018943
24. Thomas NL, Windle AH. A deformation model for Case II diffusion. Polymer (Guildf). 1980;21(6):613–9. https://doi.org/10.1016/0032-3861(80)90316-X
25. Tomozawa M, Lezzi PJ, Hepburn RW, Blanchet TA, Cherniak DJ. Surface stress relaxation and resulting residual stress in glass fibers: a new mechanical strengthening mechanism of glasses. J Non-Cryst Solids. 2012;358(18–19):2650–62. https://doi.org/10.1016/j.jnoncrysol.2012.06.018
26. Edwards DA, Cohen DS. A mathematical model for a dissolving polymer. AIChE J. 1995;41(11):2345–55. https://doi.org/10.1002/aic.690411102
27. Thomas NL, Windle AH. Diffusion mechanics of the system PMMA-methanol. Polymer (Guildf). 1981;22(5):627–9. https://doi.org/10.1016/0032-3861(81)90352-9

How to cite this article: Hausmann BD, Tomozawa M. Case II diffusion of water in Na_2O–$3SiO_2$ glass: Constant tensile stress gradient at the diffusion interface. Int J Appl Glass Sci. 2023;14:330–337. https://doi.org/10.1111/ijag.16622